Special Feature: Electronic and Optical Devices

Organic Field-effect Transistors Based on Graphene Fragments: Hexa-*peri*-hexabenzocoronenes

Tomohiko Mori, Hisato Takeuchi, Yoshihiro Kikuzawa and Koji Noda

■ABSTRACT‖   Hexabenzocoronene (HBC) is a hydrogen-terminated graphene fragment. Organic field-effect transistors (OFETs) based on both p-type and n-type HBC derivatives have been developed. In p-type OFETs, dihexyl (2H-HBC) and tetrahexyl (4H-HBC) derivatives that were designed to self-assemble into lamellar aggregates increased the field-effect mobilities and on/off ratios by a factor of 10 or more compared to HBC and the hexahexyl derivative, which self-assemble into columnar aggregates. 2H-HBC and 4H-HBC also have a high thermal stability. For n-type OFETs, a derivative with strong electron-withdrawing groups, hexafluorinated-HBC (6F-HBC), was synthesized. An OFET with 6F-HBC functioned as an n-type semiconductor, while one with HBC functioned as a p-type semiconductor. Hexafluoro-substitution reduced both the highest occupied molecular orbital and lowest unoccupied molecular orbital levels by 0.5 eV, which facilitated electron injection from the electrode.

Changes in the drain current caused by the presence of ethanol gas were measured, demonstrating the applicability of the present OFET devices in ethanol gas sensors. Ethanol at a concentration of 1 ppm was clearly detected, with a response time of several seconds.

■KEYWORDS‖   Organic field-effect transistor, Hexabenzocoronene, Graphene, Gas sensor, Alcohol, Ethanol

1. Introduction

Organic field-effect transistors (OFETs) have attracted considerable attention for applications such as flat-panel displays, radio-frequency tags, and chemical sensors.[1,2] Compared to FETs based on single-crystalline inorganic semiconductors such as Si, SiC, GaAs, and GaN, those based on single-crystalline organic semiconductors have significantly lower carrier mobility. Carrier mobility as high as 35 cm^2/Vs at room temperature was measured in single crystals of pentacene, which is the highest value among organic semiconductors.[3] Consequently, OFETs are not suitable for use in applications requiring very high switching speed or high power. Due to the unique processing capabilities of OFETs, such as low-temperature formation, screen printing, and inkjet printing, however, OFETs can be competitive candidates for FET applications requiring light weight, low cost, large area, and/or flexibility. Such applications include switching devices for organic electroluminescence displays, liquid crystal displays, smart cards, and radio-frequency tags.[1] In thin-film

based OFETs, carrier mobilities of 5 cm^2/Vs have been reported in pentacene.[4] These carrier mobilities are similar to or better than those typically obtained with thin-film based FETs made from hydrogenated amorphous silicon, which have been widely used in active-matrix flat-panel displays. Additionally, the use of OFETs in chemical and biological sensors is also beginning to attract interest, because fine tuning of the chemical and physical properties is possible due to the large variety of organic semiconductors.[2]

The extended π system of organic semiconductors enhances the intermolecular overlap of π-π systems in the solid state, which leads to a relatively high mobility. Pentacene, a linear acene, is a representative organic semiconductor. A problem with linear acenes, however, is their thermal and chemical instability. Pentacene disproportionation occurs during sublimation, which is used for purification and device fabrication.[5] The development of thermally and chemically stable organic semiconductors is therefore highly desirable.

As shown in **Fig. 1**, hexabenzocoronene (HBC) can be regarded as a hydrogen-terminated graphene

fragment. Compared to linear acenes, HBC is thermally and chemically stable. HBC derivatives also maintain a very high chemical stability.[6] Because of the rich π systems of HBC, one would expect a high degree of intermolecular overlap of the π-π systems. HBC derivatives actually exhibit one of the highest intrinsic charge carrier mobilities. HBC derivatives are therefore promising candidates for organic electronic devices.[7]

A general problem with using graphene fragments such as HBC is their small grain size in thin-film form due to a low diffusion coefficient. Grain boundaries scatter carrier transport, reducing carrier mobility. HBCs introduced with peripheral alkyl chains have been reported to self-assemble into columnar aggregates,[6] as shown in **Fig. 2**. Since alkyl chains are insulating, carrier transport is facile only along the columnar axis,[7] and barriers to carrier transport exist at the grain boundaries. These alkyl-introduced HBCs have low FET mobilities of up to 10^{-3} cm^2/Vs in a thin-film sample,[8] although they display intrinsic p-type

carrier mobilities of up to 1 cm^2/Vs.[7] On the other hand, HBCs with alkyl chains introduced in two directions would self-assemble into lamellar aggregates, in which carrier transport would be easy along the layers of aromatic cores and interruptions in carrier transport would be reduced at the grain boundaries in thin films.

In addition to p-type organic semiconductors, n-type organic semiconductors are desired for the production of bipolar transistors and complimentary circuits. N-type organic semiconductors should have similar physical and electrical properties to p-type semiconductors, except for the carrier type. To date, most of the organic molecules used in OFETs have been p-type semiconductors, and only a few molecules have been found to behave as n-type semiconductors. It is known that n-type organic semiconductors require access to the lowest unoccupied molecular orbital (LUMO) level for electron injection. Therefore, molecules with strong electron-withdrawing groups are good candidates for n-type semiconductors.

In this work, HBC derivatives were synthesized as semiconductors suitable for both p-type and n-type OFETs. HBC derivatives for p-type OFETs were designed to self-assemble into lamellar aggregates. An HBC derivative with strong electron-withdrawing groups was synthesized for n-type OFETs. OFETs containing these HBC derivatives were fabricated, and their p-type and n-type semiconductor performance is presented. Changes in the drain current caused by the presence of ethanol gas were observed, demonstrating the potential of these materials for application in ethanol gas sensors.
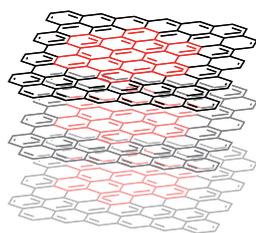
Fig. 1   HBC can be regarded as disk-shaped hydrogen-terminated graphene fragments.
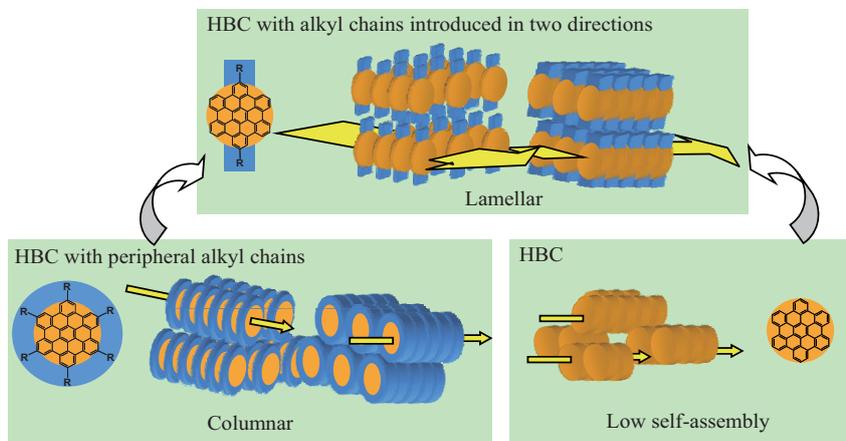
Fig. 2   Schematic molecular packing diagrams of HBC derivatives.

2. Experimental methods

The HBC derivatives investigated for use as p-type semiconductors were hexabenzocoronene, the dihexyl derivative (2H-HBC), the tetrahexyl derivative (4H-HBC), and the hexahexyl derivative (6H-HBC), as shown in **Fig. 3**. These HBC derivatives were synthesized using a previously reported method[9] with substituted starting materials. 2H-HBC and 4H-HBC were designed to form two-dimensional conducting pathways by introducing hexyl chains in two directions. A fluorinated-graphene, 2,5,8,11,14,17-hexafluorohexa-*peri*-hexabenzocoronene (6F-HBC), was also synthesized for an n-type semiconductor.

The OFET device had a top-contact structure, as shown in **Fig. 4**. A heavily doped n-type single-crystal silicon wafer (< 0.02 Ωcm) covered with a 300-nm-thick film of thermally grown silicon dioxide (SiO_2) was used as the substrate for the OFET. The silicon wafer also served as the gate electrode. The thermally grown silicon dioxide provided a good gate insulator with a high breakdown voltage and a low defect concentration. A 20-nm-thick active layer of HBC

derivatives was deposited on the SiO_2 layer by vacuum evaporation at a rate of 0.1 nm/min under a pressure of 1×10^{-5} Pa at deposition temperatures from room temperature to 150ºC. The OFETs were completed by evaporating Au (30 nm) for p-type OFETs or Ca/Al (1 nm/100 nm) layers for n-type OFETs through a shadow mask to form the source and drain electrodes, and forming a 100-nm-thick Al layer on the back side of the wafer as a contact. The channel length and width were 100 and 6000 μm, respectively. The OFET characteristics were measured using an HP4145B parameter analyzer. The n-type OFETs were annealed in a vacuum chamber at 150ºC for 1 hour to remove the influences of oxygen and humidity which would presumably trap negative carriers. The OFETs were held in a flow-through cell and exposed to controlled ethanol atmospheres, and the changes in the drain current caused by the presence of ethanol gas were measured. The ethanol concentration was controlled with flow meters by mixing dry air and 100 ppm ethanol.

The highest occupied molecular orbital (HOMO) levels of the HBC derivatives were determined using a photoelectron spectrometer (Riken Keiki Co. Ltd., AC-2) with thin-film samples. The LUMO levels were deduced from the band gaps obtained from the UV/Vis absorption spectra and the HOMO levels.

The crystal and thin-film structures were determined using powder X-ray diffraction (XRD), out-of-plane XRD, and grazing incidence X-ray diffraction (GIXD). Powder samples were sealed in a glass capillary of 0.3 mmϕ. Powder XRD data were collected at the Japan Synchrotron Radiation Research Institute (SPring-8), using beamline BL19B2, an X-ray energy of 12.4 keV, and an imaging plate. The structure and crystallinity of the thin films were characterized by out-of-plane

(a) HBC   (b) 2H-HBC   (c) 4H-HBC

(d) 6H-HBC   (e) 6F-HBC
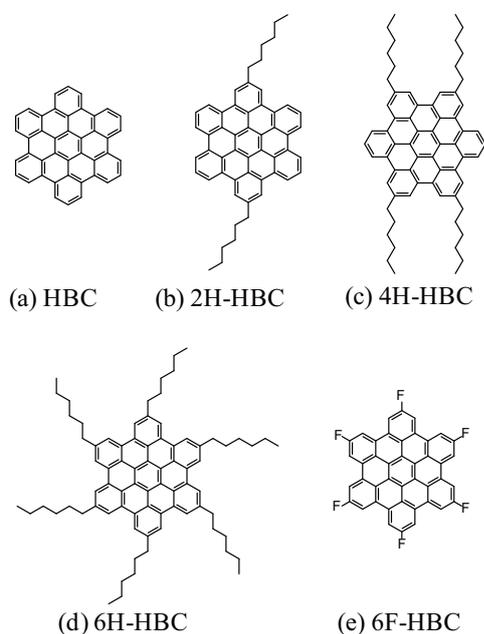
Fig. 3 Molecular structures of the HBC derivatives investigated. (a) Hexa- *peri*-hexabenzocoronene (HBC), (b) 2,11-Dihexyl-hexa-*peri*-hexabenzocoronene (2H-HBC), (c) 2,5,11,14-Tetrahexyl-hexa-*peri*-hexabenzocoronene (4H-HBC), (d) 2,5,8,11,14,17-Hexahexyl-hexa-*peri*-hexabenzocoronene (6H-HBC), (e) 2,5,8,11,14,17-hexafluoro-hexa-*peri*- hexabenzocoronene (6F-HBC).
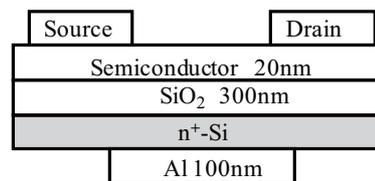
Fig. 4 Schematic structure of the OFET devices investigated in this study. The semiconductor materials and source/drain electrodes were HBC, 2H-HBC, 4H-HBC, 6H-HBC, and Au (30 nm) for p-type, and 6F-HBC and Al (100 nm) / Ca (1 nm) for n-type, respectively.

XRD and GIXD. Out-of-plane XRD (θ-2θ) scans were acquired using a Rigaku RINT 2200 system with Cu-Kα radiation. GIXD was performed at SPring-8, using beamline BL46XU at an incident angle of 0.13° and an X-ray energy of 12.0 keV.

3. Results and discussion

3. 1 P-type organic semiconductor

Figure 5 shows the output and transfer characteristics of a typical OFET based on a 2H-HBC active layer. The application of a negative voltage to the gate increased the negative drain current, indicating that the FET with 2H-HBC performed as a p-type transistor and was an enhancement-mode device. OFETs based on HBC, 4H-HBC, and 6H-HBC also showed p-type and enhancement-mode characteristics. The field-effect mobilities were calculated using the I_D values in the saturation regions. The field-effect mobilities and on/off ratios for all of the HBC derivatives are summarized in **Table 1**. Compared to

HBC and 6H-HBC, 2H-HBC and 4H-HBC had extremely high field-effect mobilities.[10] The mobilities were increased by about one order of magnitude after introducing alkyl groups in two directions. 2H-HBC and 4H-HBC also had higher on/off ratios.

The thermal stability of the OFETs was investigated on the basis of the temperature dependence of the carrier mobility of OFETs containing HBC derivatives. As shown in **Fig. 6**, the carrier mobility of 2H-HBC did not drop until 100ºC, that of 4H-HBC slightly decreased with increasing temperature, and that of 6H-HBC decreased with increasing temperature. The decrease of carrier mobility in 6H-HBC was probably related to morphology changes in the films. The increase in carrier mobility of HBC may be attributed to improved crystallinity. Our results indicate that 2H-HBC and 4H-HBC had a high thermal stability.

To examine these hypotheses, crystal and thin-film structures were examined using powder XRD, out-of-
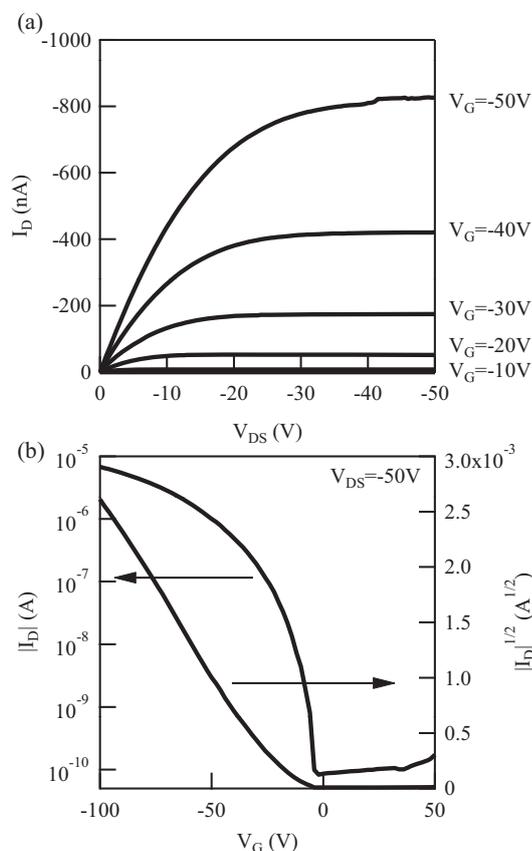
Fig. 5 Output (a) and transfer (b) characteristics of a 2H-HBC FET.

Table 1 Field-effect mobilities and on/off ratios of HBC derivatives measured at room temperature.

Compound	Mobility (cm^2/Vs)	On/off ratio
HBC	1.4×10^{-4}	330
2H-HBC	1.1×10^{-2}	82000
4H-HBC	1.2×10^{-2}	57000
6H-HBC	9.5×10^{-4}	870
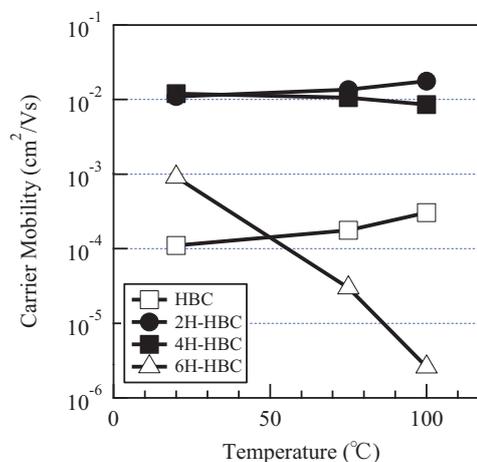
Fig. 6 Temperature dependence of the carrier mobility in OFETs of HBC derivatives.

plane XRD, and GIXD. **Figure 7** shows out-of-plane XRD (θ-2θ) and GIXD patterns of HBC derivatives deposited at room temperature on SiO_2/Si substrates. The XRD patterns contained Bragg reflections, all of whose indices were assigned to the c-plane, indicating that the films were textured. The layer spacings (d_{001}) determined from the out-of-plane XRD patterns, and the in-plane lattice parameters (a, b) and the angle between them (γ) determined from the GIXD patterns are presented in **Table 2**. **Figure 8** shows molecular packing diagrams for 2H-HBC determined by the

Table 2 Comparison of unit cell dimensions in HBC derivative films.

Compound	a (nm)	b (nm)	d_{001} (nm)	γ (deg)
HBC	-	-	1.21	-
2H-HBC	1.875	0.505	1.86	90
4H-HBC	1.970	0.501	2.34	90
6H-HBC	-	-	1.75	-
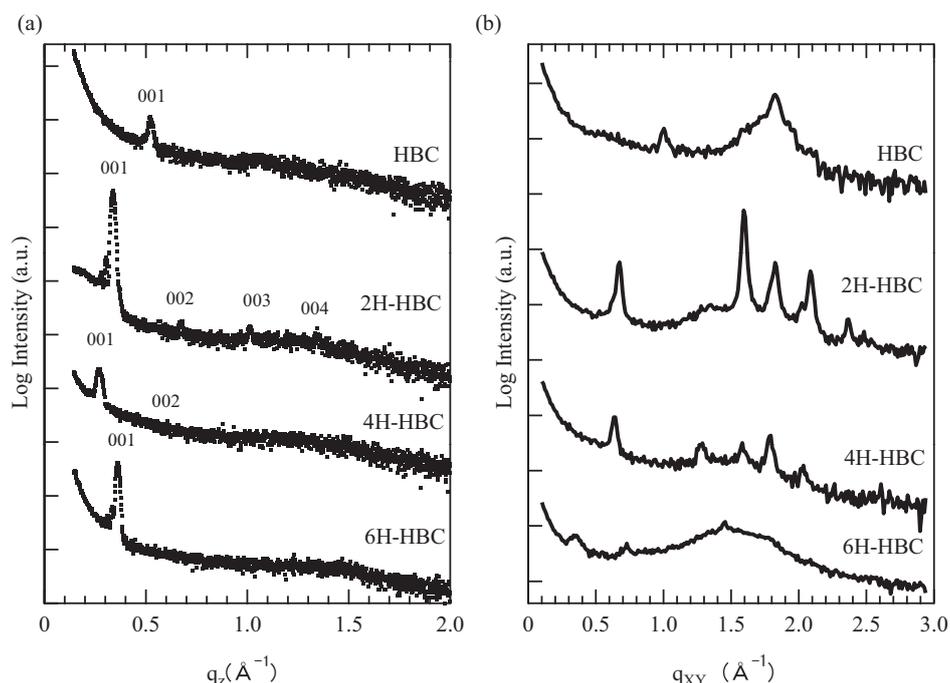
Fig. 7 Out-of-plane XRD patterns (a) and GIXD patterns (b) of HBC derivatives deposited on SiO_2/Si substrates.
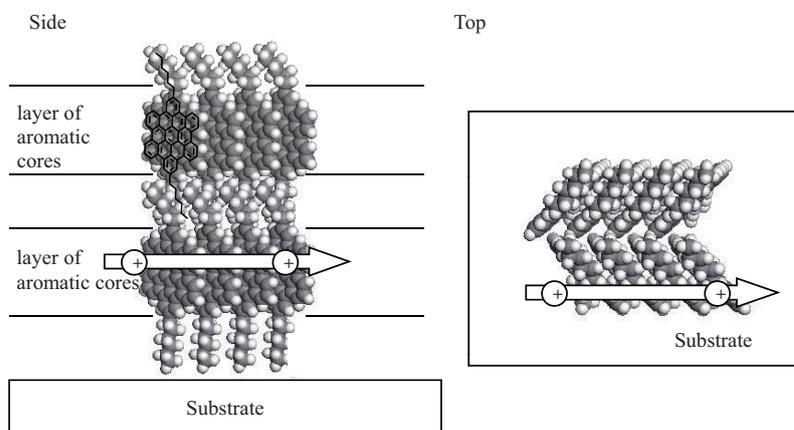
Fig. 8 Molecular packing diagram of 2H-HBC.

software package Reflex Plus, which is based on the Power Solve approach.[11] As expected, the films of 2H-HBC self-assembled into lamellar aggregates; that is, with layers of aromatic cores lying parallel to the substrate.[12] Since the XRD patterns of 4H-HBC were similar to those of 2H-HBC, these two derivatives probably had a similar film structure. HBC has small grains in thin films due to its low diffusion coefficient, and grain boundaries scatter carrier transport and reduce mobility. 6H-HBC self-assembles into columnar aggregates,[6] in which carrier transport should be broken at the grain boundaries in the thin film. 2H-HBC and 4H-HBC self-assembles into lamellar aggregates, in which carrier transport is easy along the layers of aromatic cores, and in which interruptions in carrier transport are reduced at the grain boundaries in thin film. Therefore, the high carrier mobilities and on/off ratios of the 2H-HBC and 4H-HBC films can be attributed to lamellar aggregation, in contrast to the columnar aggregation of 6H-HBC.

3. 2 N-type organic semiconductor

Figure 9 shows the output and transfer characteristics of OFET fabricated from a 6F-HBC active layer. The application of a positive voltage to the gate increased the positive drain current. This indicates that the OFET fabricated from 6F-HBC performed as an n-type transistor,[13,14] in contrast to the p-type HBC transistor.[10] The field-effect mobilities were calculated using the I_D values in the saturation regions. The electron field-effect mobility and on/off ratio for 6F-HBC were 1.6×10^{-2} cm²/Vs and 10^4, respectively.

The electron mobility of 6F-HBC was comparable to the hole mobilities of 2H-HBC and 4H-HBC.

The LUMO levels of HBC and 6F-HBC were 2.7 eV and 3.2 eV, respectively. Therefore, hexafluoro-substitution reduced the LUMO level by 0.5 eV that facilitated electron injection from the electrode.

Powder XRD, out-of-plane XRD, and GIXD were performed to study the thin-film structure of 6F-HBC. The calculated thin-film structure is shown in **Fig. 10**. Interestingly, because of the large van der Waals radius of fluorine, 6F-HBC has a face-to-face structure, while HBC has a herringbone structure.[15] Curtis and co-workers recently performed a structural analysis of
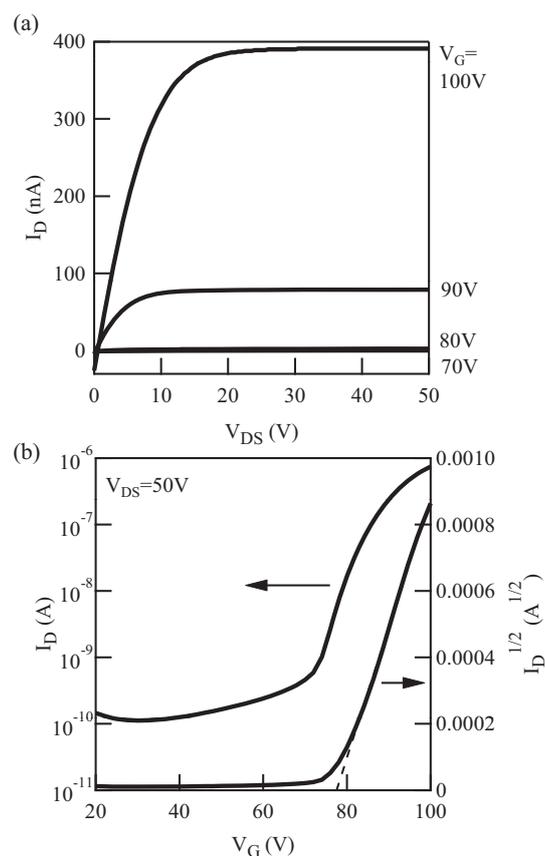
Fig. 9 Output (a) and transfer (b) characteristics of a 6F-HBC OFET.
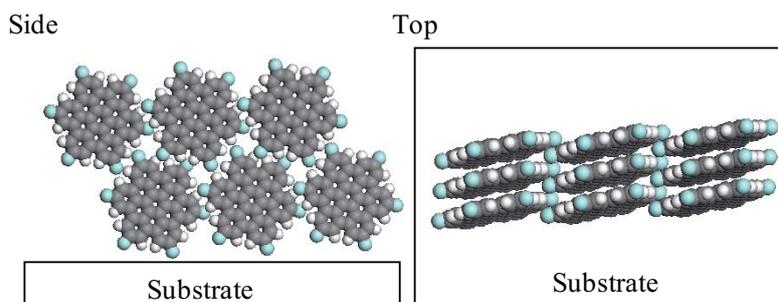
Fig. 10 Molecular packing diagram of 6F-HBC.

some common organic semiconductors, discussing the correlation between solid-state packing and transport.[16] Theoretically, a face-to-face structure is expected to provide more efficient orbital overlap, and thereby facilitate carrier transport. Therefore 6F-HBC has a preferable crystal structure for carrier transport.

3. 3 Ethanol sensing capability

The presence of polar molecules is known to decrease the rate of charge transport in organic materials by increasing energetic disorder through charge-dipole interactions.[17,18] **Figure 11** shows the relative percentage responses evaluated from the drain transient current variation. An OFET based on 2H-HBC was exposed to a flow of ethanol diluted by dry air. The concentrations of ethanol were in the range from 1 to 100 ppm. The presence of ethanol resulted in a decrease in the drain current.[19] Ethanol at a level of 1 ppm was clearly detectable, with a response time of several seconds.

4. Conclusion

OFETs fabricated from both p-type and n-type HBC derivatives were developed. As p-type semiconductors, 2H-HBC and 4H-HBC were designed to form two-dimensional conducting pathways by introducing hexyl chains in two directions. OFETs based on 2H-

HBC and 4H-HBC had extremely high field-effect mobilities compared to those based on HBC and 6H-HBC. XRD results suggested that this enhanced performance can be explained by the lamellar aggregation of the HBC derivatives. 2H-HBC and 4H-HBC also had a high thermal stability.

OFETs containing 6F-HBC performed as n-type transistors. The electron field-effect mobility and on/off ratio for 6F-HBC were 1.6×10^{-2} cm^2/Vs and 10^4, respectively. The electron mobility of 6F-HBC was comparable to the hole mobilities of 2H-HBC and 4H-HBC. The large van der Waals radius of fluorine leads to a change in the crystal structure of 6F-HBC from herringbone to face-to-face, which is a preferable structure for carrier transport.

Changes in the drain current caused by ethanol gas were measured. The presence of ethanol resulted in a decrease in the drain current. Ethanol at 1 ppm was clearly detected, with a response time of several seconds. These OFETs could be used in inexpensive alcohol sensors to help prevent automobile accidents caused by alcohol-impairment.

Fig. 11 Relative percentage responses evaluated from the drain transient current variation measured at a gate voltage of −5 V and a drain voltage of −5 V. An OFET with 2H-HBC was exposed to air containing different concentrations of ethanol.

References

(1) Dimitrakopoulos, C. D. and Malenfant, P. R. L., "Organic Thin Film Transistors for Large Area Electronics", *Adv. Mater.*, Vol.14, No.2 (2002), pp.99-117.
(2) Robert, M. E., et al., "Materials and Device Considerations for Organic Thin-film Transistors Sensors", *J. Mater. Chem.*, Vol.19, No.21 (2009), pp.3351-3363.
(3) Jurchescu, O. D., et al., "Effect of Impurities on the Mobility of Single Crystal Pentacene", *Appl. Phys. Lett.*, Vol.84, No.16 (2004), pp.3061-3063.
(4) Kelly, T. W., et al., "Recent Progress in Organic Electronics: Materials, Devices, and Processes", *Chem. Mater.*, Vol.16, No.23 (2004), pp.4413-4422.
(5) Roberson, L. B., et al., "Pentacene Disproportionation during Sublimation for Field-Effect Transistors", *J. Am. Chem. Soc.*, Vol.127, No.9 (2005), pp.3069-3075.
(6) Herwig, P., et al., "Columnar mesophases of Alkylated hexa-*peri*-hexabenzocoronenes with Remarkably Large Phase Widths", *Adv. Mater.*, Vol.8, No.6 (1996), pp.510-513.
(7) Van de Craats, A. M., et al., "Record Charge Carrier Mobility in a Room-temperature Discotic Liquid-crystalline Derivative of Hexabenzocoronene", *Adv. Mater.*, Vol.11, No.17 (1999), pp.1469-1472.
(8) Van de Craats, A. M., et al., "Meso-epitaxial Solution-growth of Self-organizing Discotic Liquid-crystalline Semiconductors", *Adv. Mater.*, Vol.15,

No.6 (2003), pp.495-499.

(9) Watson, M. D., et al., "Big is Beautiful-"Aromaticity" Revisited from the Viewpoint of Macromolecular and Supramolecular Benzene Chemistry", *Chem. Rev.*, Vol.101, No.5 (2001), pp.1267-1300.

(10) Mori, T., et al., "Field-effect Transistors Based on a Polycyclic Aromatic Hydrocarbon Core as a Two-dimensional Conductor", *J. Appl. Phys.*, Vol.97, No.6 (2005), p.066102.

(11) *Materials Studio* (version 3.2) (2005), Accelrys Inc., San Diego.

(12) Mori, T., et al., "Transistor Performance and Film Structure of Hexabenzocoronene Derivatives", *Mater. Res. Soc. Symp. Proc.*, Vol.1091 (2008), 1091-AA11-41.

(13) Kikuzawa Y., et al., "Synthesis of 2,5,8,11,14,17-Hexafluoro-hexa-*peri*-hexabenzo-coronene for n-Type Organic Field-effect Transistors", *Org. Lett.*, Vol.9, No.23 (2007), pp.4817-4820.

(14) Mori, T., et al., "N-type Field-effect Transistor Based on a Fluorinated-graphene", *Org. Electron.*, Vol.9, No.3 (2008), pp. 328-332.

(15) Goddard, R., et al, "Crystallization of Large Planar Polycyclic Aromatic Hydrocarbons: The Molecular and Crystal Structures of Hexabenzo[bc, ef, hi, kl, no, qr]coronene and Benzo [1,2,3 -bc:4,5,6-b'c'] dicoronene", *J. Am. Chem. Soc.*, Vol.117 (1995), pp.30-41.

(16) Curtis, M., et al., "Solid-state Packing of Conjugated Oligomers: From π-Stacks to the Herringbone Structure", *J. Am. Chem. Soc.*, Vol. 126 (2004), pp.4318-4328.

(17) Dunlap, D. H., et al., "Charge-dipole Model for the Universal Field Dependence of Mobilities in Molecularly Doped Polymers", *Phys. Rev. Lett.*, Vol.77, No. 3 (1996), pp.542-545.

(18) Novikov, S. V., et al., "Essential Role of Correlations in Governing Charge Transport in Disordered Organic Materials", *Phys. Rev. Lett.*, Vol.81, No.20 (1998), pp.4472-4475.

(19) Mori, T., et al., "Improving the Sensitivity and Selectivity of Alcohol Sensors Based on Organic Thin-Film Transistors by Using Chemically-Modified Dielectric Interfaces", *Proc. of IEEE Sensors 2009 Conference* (2009), pp.1951-1954, IEEE.

Tomohiko Mori
  Research Field :
    - Organic electronics
  Academic Degree : Dr. Sci.
  Academic Society :
    - The Japan Society of Applied Physics

Takeuchi Hisato
  Research Fields :
    - Organic synthesis
    - Adhesive materials
  Academic Degree : Dr. Eng.
  Academic Societies :
    - American Chemical Society
    - The Chemical Society of Japan
    - The Adhesion Society of Japan

Yoshihiro Kikuzawa
  Research Field :
    - Organic chemistry (Adhesive, Functional organic materials)
  Academic Degree : Dr. Sci.
  Academic Societies :
    - The Chemical Society of Japan
    - The Society of Synthetic Organic Chemistry, Japan

Koji Noda
  Research Field :
    - Organic electronics
  Academic Societies :
    - The Japan Society of Applied Physics
    - Society of Automotive Engineers of Japan